ACTA METALLURGICA SLOVACA
2023, VOL. 29, NO. 2, 59-62

RESEARCH PAPER

EFFECT OF (Al, Zn, Cu, AND Sr) DOPING ON STRUCTURAL, OPTICAL AND ELECTRICAL PROPERTIES OF SPRAYED SnO_2 THIN FILMS

Imene Saoula[1], Chahinez Siad[1], Khedidja Djedidi[1], Nassiba Allag [1], Abdelouahad Chala[1]

[1]Physics Laboratory of Thin Films and Applications (LPCMA), University of Biskra, 07000, Algeria

*Corresponding author: imene.saoula@univ-biskra.dz, tel.: 0664733569, Department of material science faculty, University of Biskra, BP 145 RP, 07000 Biskra, Algeria

Received: 15.02.2023
Accepted: 04.04.2023

ABSTRACT

Tin dioxide thin films deposited onto a glass substrate were prepared by spray pyrolysis technique, and then doped with different elements which are: Al, Zn, Cu, and Sr by electroplating method, these elements were chosen for their different atomic radii. XRD illustrate that all the films were polycrystalline with a tetragonal rutile structure and a strong preferred orientation of (200) plane. Uv-vis spectrophotometer specters showed that the highest average transmittance of Al/SnO_2 film was about 86.77% in the visible region and the Sr/SnO_2 film had the highest band gap of 3.95 eV. From the MEB images, the morphological characteristics improved when the SnO_2 thin films doped with Al and Zn but the opposite happened when it doped with Cu and Sr. The four-point probe showed that the best sample was for Al/SnO_2 because it had the highest electrical conductivity around 692.306 $(\Omega.cm)^{-1}$.

Keywords: Thin films; SnO2; Optical properties; Electrical properties; Structural properties; Morphological properties

INTRODUCTION

Thin films of transparent conductive oxide such as ZnO [1], TiO2[2], In_2O_3 [3], and SnO_2[4], are the most scientific research subjects in current applications, and the most common is SnO_2 due to its large band gap (3.65 V at 300 K) [5] making it the most widely used in many applications such as a transparent electrode in photovoltaic transformers, amorphous silicon solar cells, liquid crystal display and gas-discharge display [6]. It can be deposited by a number of mechanisms such as spraying pyrolysis [7], L-CVD [8] spin coating [9], theoretically the SnO_2 thin film has a low electrical conductivity because its charge carriers have low mobility as well as its low-density charge carrier [5], which leads us to dope it with many elements to improve the most important physical properties, namely the electrical and optical properties, we can mention from these elements: Zr [10], Cu [11],Sb [12]…..etc.

The objective of this study is to investigate, for the first time, the influence of these four elements which have various ionic radii (r "Al^{3+}"=0.39A°, r "Zn^{2+}"=0.40A°,r "Cu^{2+}"=0.93A°, and r "Sr^{2+}"=1.16A°[13], where r "Sn^{4+}"=0.71A°[14]) on the optical and electrical properties of SnO_2 thin films, and shed more light on the structure and properties of Al, Zn, Cu and Sr-doped SnO_2 thin films. The approach is to: (i) use a simple and low-cost method (spray pyrolysis technique) to deposit SnO_2 films onto a glass substrate heated to 450 C° then doped using electroplating method, (ii) characterize their microstructural features, and (iii) measure their physical properties and correlate them with the microstructure.

MATERIAL AND METHODS

SnO2 thin films were prepared using spray pyrolysis method, tin chloride ($SnCl_2$, $2H_2O$) dissolved in bi-distilled water and methanol (1/1) with the addition of a few drops of hydrochloride (HCl) to obtain more homogenous starting solution. Then it doped choosing electroplating method at 65C° for 15 minute and in electric current between 1 and 5 mA with 0.15M of different sources for Cu, Al, Sr, and Zn, which are $CuSo_4$.$5H_2O$, $Al_2So_4.18H_2O$, $SrCl_2.6H_2O$, and $ZnCl_2.7H_2O$ respectively.

RESULTS AND DISCUSSION

Structural properties:

The structural properties of doped and undoped samples were determined using the XRD. **Fig. 1** shows that all the samples have the same preferential orientation along c-axis as pure SnO_2 it was (200) plane which determines low energy (which means the stability) because it had the highest intensity for all the films, also it had the same structure which was the tetragonal rutile [15], and there are some peaks with low intensity such as :(110), (101), (211), (310), and (301).

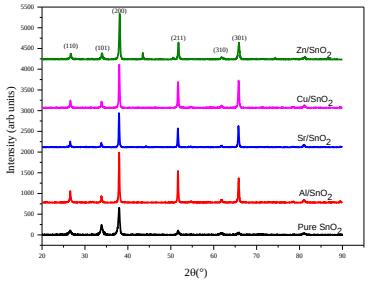

Fig. 1 X-ray diffraction spectra obtained in the film prepared with different doping.

From XRD data crystalline size was calculated according to the Scherrer formula given by D as follows [16]:

$$D=0.9\lambda/(\beta.\cos(\Theta)) \quad (1.)$$

Where λ is the X–ray wavelength (λ Kα (Cu)=1.5418 A°), β is the full width at half maximum (FWHM) and Θ is the diffraction angle, after that Williamson and Smallman's relation [17] was used to find the dislocation density:

$$\delta=1/D^2 \quad (2.)$$

From **Table 1** we can observe that Al/SnO_2 has the highest value of the crystalline size that's mean that the crystallization into the growth axe of SnO_2 thin films was improved [18], while the Sr/SnO_2 has the lowest value because the crystallization into c-axis was deterioration.

Table 1 Variation of crystalline size and dislocation density of different prepared samples.

Sample	D (nm)	$\delta*10^{-4}$ (lines/nm^2)
Pure SnO_2	35.264	8.04
Cu/SnO_2	34.251	8.52
Zn/SnO_2	42.305	5.587
Sr/SnO_2	24.548	16.6
Al/SnO_2	45.989	4.728

Morphological properties:
The MEB was used to determine the morphology of the different SnO_2 samples doped with various elements.

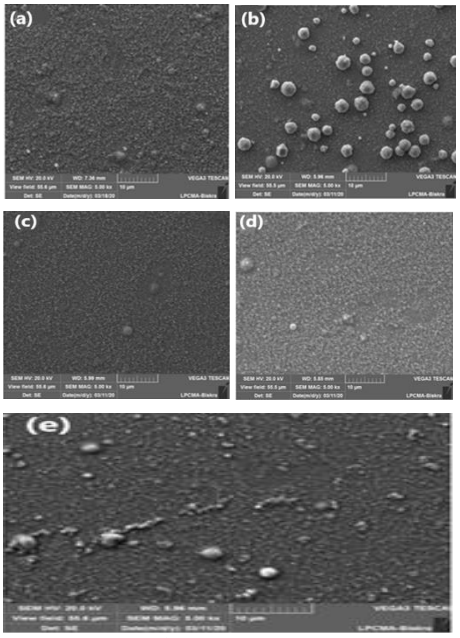

Fig. 2 MEB images of: (a) pure SnO_2, (b) Cu/SnO_2, (c) Al/SnO_2, (d) Zn/SnO_2, and (e) for Sr/SnO_2.

Firstly, **Fig. 2.b** shows Cu/SnO_2 surface morphology, we observed a spheric shape particles of negative potentials which transform copper oxide into copper was created may be because the oxide copper is placed with Cu that is mean the Cu^{2+} changed to Cu, moreover, the grain size was decreased, this consists too many studies mentioned [17,18] so adding of Cu to SnO_2 did not improve its morphology at all. The opposite was happened with the addition of Al and Zn to SnO_2 as **Fig. 2.c** and **Fig. 2.d** respectively demonstrate; this is due to the increase of grain size, which leads to the reduction of the defects in the obtained thin films. Finally, the **Fig. 2.e** (Sr/SnO_2) shows that there are black dots while for pure SnO_2 there are a few as shown in **Fig. 2.a** which mean that the defects have increased with the addition of Sr, which leads to deterioration of SnO_2 morphology.

Optical properties:

The optical properties of doped and undoped SnO_2 thin films were characterized using a UV-vis spectrophotometer in the range of [300nm-1100nm].
From **Fig. 3**, we observed that the transmittance was enhanced for Al/SnO_2 and Zn/SnO_2 (86.77% and 83.00% respectively while for pure SnO_2 was 76.91%), but for Cu/SnO_2 and Sr/SnO_2 the transmittance was decreased to 75.00% and 67.98% respectively.

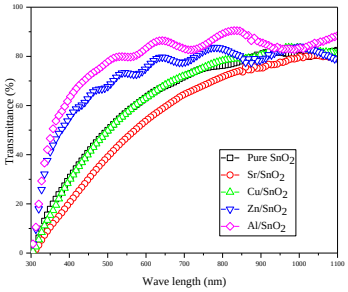

Fig. 3 Transmission spectra as a function of wavelength for undoped and doped SnO_2 thin films.

To find the band gap value (E_g) we use the Tauc model known with the following relationship [21]:

$$\alpha h v=A (h v-E_g)^{(1/2)} \quad (3.)$$

Fig. 4 ,shows the different band gap values , an increase in E_g was observed for Cu/SnO_2 and Sr/SnO_2 from 3.84 eV for pure SnO_2 to 3.94 eV and 3.95 eV respectively this increased may be due to the presence of active transition involving levels; this leads to the reduction of the conduction band (CB) and valence band (VB) and causes an up-down movement of E_c and E_v respectively, the same phenomena are carried by Talal and al ,they observed a blue shift of the absorption edges from 3.33 eV to 4.13 eV [22]. But the E_g value decreased to 3.82 eV and 3.77 eV for Zn/SnO_2 and Al/SnO_2 respectively, this is probably due to the valence band conduct

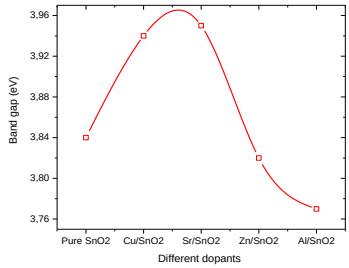

Fig. 4 Variation of optical band gap values for undoped and doped SnO_2 thin films.

Electrical properties:

The electrical properties of our films were investigated using four-point probe, the results are shown in **Table 2**:

Table 2 Electrical properties of pure and doped SnO_2.

	ρ (Ω.cm) *10-3	σ*10²(Ω.cm)⁻¹
SnO_2	1.84	5.41
Cu/SnO_2	2.36	4.22
Zn/SnO_2	1.59	6.28
Sr/SnO_2	3.28	3.04
Al/SnO_2	1.44	6.92

The following relations was applied [16] to determine the sheet resistance (R_s), the electrical resistivity (ρ), and the electrical conductivity (σ).

$$R_s=F.(V/I) \quad (4.)$$
$$\rho=R_s.\,d \quad (5.)$$
$$\sigma=1/\rho \quad (6.)$$

Where F=4.532 is the correction factor, 'I' the applied current, 'V' is the measured voltage, and 'd' is the film thickness.
As is seeing, the electrical conductivity of Sr/SnO_2 and Cu/SnO_2 was decreased compared to pure SnO_2, this result can be interpreted by the decrease in the number of charge carriers [24], so the so existence of a difference in the structure of Cu and SnO_2 or Sr and SnO_2 abstract the flow of the electrons [25], also the grain size decreased as we found in Table.1 hence to that there are more grain boundaries which are limiting the mobility of electrons (acts as traps for free carriers and as barriers against transport) which may be responsible for the increase in the electrical resistivity, Sudip Kumarsinla study revealed the same result [26].
The opposite happened for Zn/SnO_2 and Al/SnO_2, the decrease in the resistivity which can be attributed to the increase in the number of free charge carrier from the donor Zn^{2+} or Al^{3+} ions that incorporated into the substitutional or interstitial cation location of Sn^{4+} [15].
From Fig.5, Al/SnO_2 has the highest value of the electrical conductivity (6,923*10² (Ω.cm)⁻¹).

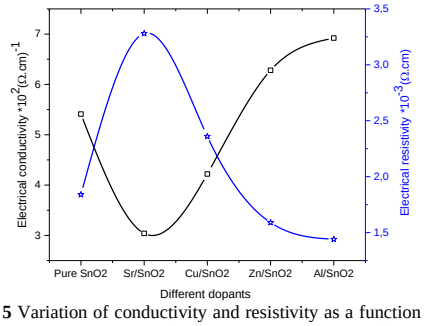

Fig. 5 Variation of conductivity and resistivity as a function of different dopant elements of pure and doped SnO_2 thin film.

CONCLUSIONS

Smooth, dense, continuous, and homogenous undoped and (Al, Zn, Cu and Sr) doped SnO_2 thin films were successfully deposited onto a glass substrate heated to 500 C° using a simple and low-cost spray pyrolysis technique. The films were polycrystalline and had a tetragonal rutile structure with preferred growth orientation along <200> direction. The band gap of pure SnO_2 (3.84 eV) decreased to 3.82 and 3.77 eV as a result of doping with Zn and Al, respectively; and increased to 3.94 eV and 3.95 eV because of doping with Cu and Sr, respectively. Doping SnO_2 with Al and Zn increased its crystalline size and improved its optical transmittance, but the opposite was happened when it doped with Cu and Sr. Aluminium and zinc increased the electrical conductivity of SnO_2 from 5.41*10² (Ω.cm)⁻¹ to 6.92*10² (Ω.cm)⁻¹ and 6.28*10²(Ω.cm)⁻¹, respectively, but Strontium and Copper decreased it to 3.04*10² and 4.22*10² (Ω.cm)⁻¹ respectively.

REFERENCES

1. W. Allag, H. Guessas, M. Hemissi, M. Boudissa: Optik, 2019, 2020, 165287. https://doi.org/10.1016/j.ijleo.2020.165287.
2. H. Attouche, S. Rahmane, S. Hettal, N. Kouidri: Optik, 203, 2020, 163985. https://doi.org/10.1016/j.ijleo.2019.163985.
3. M. Ghemid , H. Gueddaoui, M. Hemissi, M.R. Khelladi, R. Bourzami: Chemical Physics Letters, 784, 2021, 139089. https://doi.org/10.1016/j.cplett.2021.139089.
4. P. Sivakumar, H. S. Akkera, T. R. K. Reddy, G. S. Reddy, N. Kambhala, N. N. K. Reddy: Optik, 226, 2021, 165859. https://doi.org/10.1016/j.ijleo.2020.165859.
5. L. Soussi, T. Garmim, O. Karzazi, A. Rmili, A. El Bachiri, A. Louardi, H. Erguig: Surfaces and Interfaces, 19, 2020, 100467. https://doi.org/10.1016/j.surfin.2020.100467.
A. Abdelkrim, S. Rahmane, O. Abdelouahab, N. Abdelmalek, Gasmi Brahim: Optik, 127, 2016, 2653-2658. http://dx.doi.org/10.1016/j.ijleo.2015.11.232.
B. Khelifi, A. Attaf: Surfaces and Interfaces, 18, 2020, 100449. https://doi.org/10.1016/j.surfin.2020.100449.
6. J. Szuber, G. Czempik, R. Larciprete, B. Adamowicz: Sensors and Actuators B, 70, 2000, 177–181. https://doi.org/0.1016/S0925-4005(00)00564-5.
7. S.S. Soumya, T.S. Xavier: Physica B, 624, 2022, 413432. https://doi.org/10.1016/j.physb.2021.413432.
8. X. Zhang, X. Liu , H. Ning, W. Yuan, Y. Deng, X. Zhang, S. Wang, J. Wang, R.Yao, J. Peng: Superlattices and Microstructures, 123, 2018, 330-337. https://doi.org/10.1016/j.spmi.2018.09.016.
9. S. I. Abbas, S. F. Hathot , A. S. Abbas , A.A. Salim: Optical Materials, 117, 2021, 111212. https://doi.org/10.1016/j.optmat.2021.111212.
10. Md. F. Hossain, Md. Abdul H. Shah, Md. A.Islam, Md. S.Hossain: Materials Science in Semiconductor Processing, 121, 2021, 105346 https://doi.org/10.1016/j.mssp.2020.105346.
11. L. Bergerot : *Etude de l'élaboration d'oxyde transparent conducteur de type-p en couches minces pour des applications à l'électronique transparente ou au photovoltaïque*, 2015, Grenoble Alpes university.
12. S. Roguai, A. Djelloul: Inorganic Chemistry Communications, 138, 2022, 109308. https://doi.org/10.1016/j.inoche.2022.109308.
13. S. M.-M. Berson : *Synthèse, caractérisation et nanostructuration de dérivés du polythiophène pour des applications en cellules photovoltaïques organiques*, 2007, Joseph-Fourier-Grenoble I university.
14. R. Ramarajan, M. Kovendhan, K. Thangaraju, D. P. Joseph, R. R. Babu, V. Elumalai: Journal of Alloys and Compounds, 823, 2020, 153709. https://doi.org/10.1016/j.jallcom.2020.153709.
15. C. Khelifi, A. Attaf, H. Saidi, A. Yahia, M. Dahnoun: Surfaces and Interfaces, 15, 2019, 244-249.

https://doi.org/10.1016/j.surfin.2019.04.001.
16. N. Oleksiy : *Synthèse: Simulation, fabrication et analyse de cellules photovoltaïques à contacts arrières interdigités*, 2007, Electronics, Electro-technical and Automatic school.
17. B. Liu, H. C. Zeng: Journal of the American Chemical Society, 126, 2004, 244, 16745.
https://doi.org/10.1021/ja044825a.
18. S. Y. Lee, E. S. Shim, H. S. Kang, S. S. Pang, J. S. Kang: Thin Solid Films, 473, 2005, 31-34.
https://doi.org/ 10.1016/j.tsf.2004.06.194.
19. E. F. Keskenler, G. Turgut , S. Dogan: Superlattices and Microstructures, 52, 2012, 107-115.
http://dx.doi.org/10.1016/j.spmi.2012.04.002.
20. S. Goldsmith, E. Çetinörgü , R.L. Boxman: Thin Solid Films, 517, 2009, 5146–5150.
http://dx.doi.org/10.1016/j.tsf.2009.03.019.
21. B. Teldja, B. Noureddine, B. Azzeddine, T. Meriem: Optik, 209, 2020, 164586. https://doi.org/10.1016/j.ijleo.2020.164586.
22. J. Elias, R. Tena-Zaera, C. Lévy-Clément: Thin Solid Films, 515, 2007, 8553–8557.
https://doi.org/ 10.1016/j.tsf.2007.04.027.
23. R. T. Zaeraa, A. Katty, S. Bastide, C. Levy-Clement, B. O'Regan, V. Munoz-Sanjosé: Thin Solid Films, 483, 2005, 372–377. https://doi.org/ 10.1016/j.tsf.2005.01.010.
24. A.A. Yada, E.U. Masumdar, A.V. Moholkar, M. Neumann-Spallart, K.Y. Rajpure, C.H. Bhosale: Journal of Alloys and Compounds, 488, 2009, 350–355.
https://doi.org/ 10.1016/j.jallcom.2009.08.130.